SAND80-1904

STRUCTURAL ANALYSIS OF THE WEST HACKBERRY #6

SPR STORAGE CAVERN

UC-94

S. E. BENZLEY, 5522

SUMMARY

Four separate structural analyses of the West Hackberry #6 SPR storage cavern are presented. One analysis covers the creep response of the cavern beginning shortly before the time when an accidental fire occurred and proceeding through the cavern recertification pressure test. The second analysis models the surface uplift-that is expected during the same pressure test. The third and fourth numerical studies investigate the structural response of West Hackberry #6 to slabbing and a rapid pressure drop. All analyses indicate that this cavern should be structurally stable for the conditions assumed.

1. Introduction

The-Energy Policy and Conservation Act of 1975 authorizes the creation of a Strategic Petroleum Reserve (SPR) of up to one billion barrels of oil. One of the basic problems of such a reserve is the procurement of adequate storage facilities. The initial criteria for the selection of the storage media were the time required for development, cost, safety, environmental acceptability, and distributional capability. This criteria led to the selection of several salt dome sites in the Gulf Coast region of the U. S. that had existing solution mined caverns and large salt mines in which oil could readily be stored. The specific storage facility addressed in this report is cavern #6 at the West Hackberry salt dome, (i.e., WH 6) Cameron Parish, Louisiana.

Figure 1 is a map of the West Hackberry field showing the contours of the top of the salt. A geological cross-section of this dome taken through section B - B' of Figure 1 is given in Figure 2. The specific location of cavern number 6 in a plan view is shown in Figure 3. A more comprehensive characterization of this particular geological structure may be found in Reference 1. The early sonar surveys of WH 6 indicated a cavern profile as shown in Figure 4 [2]. However, more recent sonar work has shown that WH 6 actually has the shape as shown in Figure 5 [3]. Stress analyses on both of the above mentioned cavern shapes are given in a later section of this report.

One of the major structural reliability concerns of this specific storage facility is the non-optimum "pancake" shape of the cavern. This structural form has the potential for large vertical roof motions near the cavern centerline. Added concerns about WH 6 were realized when a serious accident occurred at the well head resulting in a fire and loss of life. Because of this accident, both the complete evacuation of the oil already in storage in the cavern and another pressure certification of this facility were required.

Four finite element models of WH 6 have been analyzed. The first of these calculations studies the 2 year creep response in the immediate vicinity of the cavern. This analysis provides a model of the creep closure of the cavern as well as the elastic response of the cavern during the recertification pressure tests. Specific information calculated includes: 1) cavern volume change during recertification, 2) stress change, during recertification, and 3) long term cavern roof motion.

The second set of calculations models a two dimensional cross-section of the West Hackberry salt dome. This simple elastic solution attempts to include the effects of the salt, caprock, a silty clay overburden, the edge effect of the dome, and the location of cavern #6 on the surface displacement during cavern pressurization. Specific information calculated

from this model includes: 1) surface uplift during recertification, 2) surface tilt during recertification and 3) the effect of various elastic properties on the total dome response.

The third analysis simulates the effects of slabbing failure. This elastic analysis shows the structural response and resulting stress state changes when a predetermined amount of the WH 6 roof is assumed to slab off.

The fourth analysis models the instantaneous (elastic) changes in stress state assuming an accident occurs that significantly reduces the cavern pressure. Such a condition may occur, for example, if one of the oil injection strings failed and the cavern pressure dropped from the brine head of 1766 psi to the oil head of 1163 psi.

2. Cavern Creep Model

In this analysis an axisymmetric model of WH 6, free from the effects of adjacent caverns was assumed. The MARC [4] finite element program was used to perform the calculations. The creep response of the salt is represented in the MARC calculation by a primary creep law presented by Hansen [5] for the salt from the Jefferson Island, Louisiana dome and from the Lyons Kansas site. This particular creep model was chosen to address relatively short term effects. The relationship between the axial creep strain and the stress and time for the tests conducted by Hansen is written as:

$$\epsilon = A\,\sigma^{m} t^{n} \qquad (1)$$

where t is the time in seconds, and σ is the differential axial stress in psi. A strain hardening form of this law was used in the MARC code. For the Jefferson Island salt the parameters in the creep law are

$$\begin{aligned} A &= 3.4 \times 10^{-13} \\ m &= 2.5 \\ n &= 0.38 \end{aligned} \qquad (2)$$

The parameters used for the Lyons, Kansas salt are

$$A = 1.53 \times 10^{-15}$$
$$m = 3.0$$
$$n = 0.4 \qquad (3)$$

Note that these two relationships are written for ambient temperature whereas the creep behavior of salt is strongly dependent upon temperature.(2) The temperature of the salt cavern is most likely higher than ambient conditions; thus the actual creep response of the cavern may be greater than the numerical results. These calculations are, however, useful in predicting the trends in creep behavior. The elastic or instantaneous response is not as dependent upon temperature, thus these results should give more accurate absolute magnitudes.

The elastic constants for salt used in this analysis were

Young's Modulus, $E = 5.76\ (10)^8$ psf

Poisson's Ratio, $\nu = .22$

Figure 6 shows a schematic diagram of the depth of cavern #6 and the separate layers of oil and water in the cavern. The two finite element grids used in this study are shown in Figure 7. Figure 7a models the cavern shape indicated by early sonar surveys and Figure 7b models the cavern shape as determined by more recent surveys.

The outer vertical boundary of each finite element model is 1200 feet from the cavern centerline. This boundary is constrained such that each boundary node will have equal lateral motion. A horizontal stress equal to the geostatic pressure of salt is applied on this boundary. The upper row of finite element nodes are also constrained to have equal vertical motion. They are loaded with a pressure equal to that produced by the overlying geologic material.

Several loading conditions to which WH 6 may be subjected are shown in Figure 8. This figure shows that the cavern certification loading is much higher than-the normal (i.e. minimum) operating pressure.* Since there is only a small change in pressure from the top to the bottom of the cavern, the pressure variation with depth is neglected.

The actual time dependent pressure history used for this study is given in Figure 9. This history simulates: 1) the pressure drop that occurred during the accident, 2) a gradual increase in cavern pressure for a year following the accident as actually recorded at the well head, 3) a bleed off of pressure to establish cavern operating conditions, and 4) the. recertification pressure excursion.

* Note that the recertification pressure excursion shown in Figure 9 also takes the cavern pressure above the maximum allowable operating pressure.

The computed vertical displacement histories at the cavern roof center point for the various shape and material models are plotted -in Figure 10. Of particular interst is the change in total cavern volume associated with the change in pressure at recertification. The result is needed to estimate the amount of fluid required to pump into the cavern to raise the pressure as required. The computed results for the cavern shape of Figure 7a indicate a cavern volume change of 76 ft^3 per psi pressure change.

Several computer plots showing equivalent creep strain and von Mises stress are given in Figures 11, 12, and 13.

3. Surface Uplift Model

This two dimensional plane strain analysis of the West Hackberry dome was undertaken to estimate the amount of surface tilt that may take place during the recertification procedure of WH 6. The problem was done using the ADINA78 [6] computer program. Only linear elastic material properties were used. The finite element grid given in Figure 13 shows the location of the three basic materials used to defined the problem. The displacement boundary conditions specified were 1) no vertical displacement on the lower surface, 2) no horizontal displacement on the side surfaces, and 3) free motion on the upper boundary. A unit normal pressure was applied to cavern surfaces.

An obvious difficulty in this particular analysis is the uncertainty that exists in defining the in situ material properties and the actual geometrical shape of the dome. This uncertainty requires that a range of material properties be used in the analysis so that the actual response may be bracketed. A list of the elastic material properties used for this problem are given in Table I. [7]

Computed ground heave profiles are shown in Figure 14 where these profiles are plotted in inches of surface displacement per psi increment of cavern pressure. It is demonstrated in Table I and Figure 14 that the elastic properties of salt strongly dominate the solution. Assuming that the actual response of the

geologic structure is bounded by the calculations, an approximation of the expected surface tilt is easily obtained from Figure 14. For example, the expected surface tilt at a point 2,000 ft. to the left of the cavern centerline would fall between $2.5\,(10)^{-8}$ and $10.0\,(10)^{-8}$ rad/psi.

Another significant correlation that is available from this calculation is the ratio of the surface displacement at the well head to the center cavern roof displacement. A tabulation of this computed ratio for the nine combinations of material properties studied is given in Table II.

An attempt was also made to model the effect of a jointed caprock region. This was done by reducing the modulus of the caprock by an order of magnitude as recommended by Voight and Dahl [8]. The results of this calculation showed negligible change in the surface displacement when compared with the results of the full value of the modulus.

4. Cavern Slabbing

This elastic axisymmetric analysis of WH 6 is an attempt to characterize the effect that a significant slabbing event would have on the post slabbed stability of the cavern. The cavern shape, initial loading, and elastic material properties are the same as those given for Figure 7b (i.e. see section 2). Roof slabbing in this calculation was modeled by "killing" six elements on the cavern roof. Note that no failure criterion was used to define this slabbing event, rather this region was just assumed to fail such that the resulting change in cavern shape could be studied. The initial loaded state on the model was the geostatic stress on the outer finite element boundaries and a brine head of 1766 psi on the cavern surfaces. Figure 15 shows the undeformed finite element model and the magnified deformed shapes of the cavern both before and after the simulated slabbing. Contours of maximum principle stresses and von Mises stresses are shown in Figures 16 and 17. Note that this simulated slabbing produced only slight changes in the global stress patterns.

5. Oil String Accident Simulation

One -possible accident that could occur that would produce a rapid decrease in the cavern pressure is the failure (i.e. rupture) of a oil injection string. This failure could cause the pressure of the cavern to drop from the brine head pressure of 1766 psi to the oil head pressure of 1163 psi. Again, the cavern shape, initial loading, and elastic material properties for the finite element model are the same as those given for Figure 7b. The effects of the postulated accident are modelled by dropping the cavern pressure from 1766 psi to 1163 psi. The magnified deformed shapes of the cavern and contours of maximum principle stress and von Mises stress are given in Figures 18, 19, and 20 respectively.

Significant changes in the global stress state around the cavern are produced by this simulated accident, however, no areas of tensile stress are created.

6. DISCUSSION

It is important to note that although the basic physics of the calculations presented here are correct and the computer programs that were used have been checked out on many problems, the results obtained are strongly dependent upon the actual way the geologic materials are modeled (i.e., the geologic constitutive models). Only a very simple creep law and linear elastic definitions were used in the problems reported here. However, even with these simple assumptions, a great deal of insight on the trends of the structural response may be obtained.

The creep closure problem demonstrated that the constitutive model for salt affected the results to greater extent than did the cavern shape. Thus accurate material models for salt are absolutely necessary for accurate creep calculational results. The surface uplift problems indicated that, even with large differences in material properties, the ratio of cavern displacement to surface displacement was essentially constant.

Significant structural events such as slabbing and rapid pressure drop appear to produce no catastrophic global cavern elastic -instabilities. Consequently, WH 6, although far from being ideal as an oil storage cavern, should remain structurally stable if subjected to the conditions assumed in this report.

Further studies of the structural stability of this and other SPR storage caverns should incorporate temperature effects on the material properties of salt.

ACKNOWLEDGEMENTS

The *author is indebted to D. W. Lobitz for initiating the creep closure calculations and to J. T. Foley for doing the material parameter study for the ground heave problem.

REFERENCES

[1] "Draft Environmental Impact Statement--Volume II." Strategic Petroleum Reserve, Texoma Group Salt Domes, National Energy Information Center, FEA/S-77/323, September 1977.

[2] "Systems Integration and Engineering Support Study for the Strategic Petroleum Reserve (SPR) Program--Final Report" SAND79-0637, Sandia Laboratories, Albuquerque, New Mexico, June 1979.

[3] Information provided by J. R. Tillerson, Sandia Laboratories.

[4] Control Data Corporation, "MARC-CDC User Information Manual Volume I, Nonlinear Finite Element Analysis Problem, Publication No. 17309500, Revision J, 1978.

[5] Hansen, F. D., "Quasi-Static Strength and Creep Differential Characteristics of Bedded Salt from the Carey Mine near Lyons, Kansas," RE/SPEC Tech. Memo Report RSI-0067 to Office of Waste Isolation, Union Carbide Corporation, Subcontract 89Y-22303C, October 1978.

[6] Bathe, Klaus-Jurgen, "ADINA--A Finite Element program for Automatic Dynamic Incremental Nonlinear Analysis," Report 82448-1, MIT, Cambridge, Mass., December 1978.

[7] Montgomery, S., memo dtd. January 3, 1980 to J. R. Tillerson, "Recommendations of Initial Simulation Models for Overburden and Caprock."

[8] Voight, B., and Dahl, H. D., "Numerical Continuum Approaches to Analysis of Nonlinear Rock Deformation," Canadian Journal of Earth Sciences, 7, 1970.

Run NO.	Clay/Silt Young's Modulus (psf)	Poisson's Ratio	Caprock Young's Modulus (psf)	Poisson's Ratio	Rock Salt Young's Modulus (psf)	Poisson's Ratio
1	$2.0(10)^5$	.33	$1.48(10)^8$	.288	$1.44(10)^8$	.22
2	$8.0(10)^5$	.33	$1.48(10)^8$	.288	$1.44(10)^8$	.22
3	$1.4(10)^6$	.33	$1.48(10)^8$	.288	$1.44(10)^8$	.22
4	$2.0(10)^5$	.33	$1.48(10)^8$	.288	$2.88(10)^8$	.22
5	$8.0(10)^5$	.33	$1.48(10)^8$	.288	$2.88(10)^8$	.22
6	$1.4(10)^6$	.33	$1.48(10)^8$	.288	$2.88(10)^8$	.22
7	$2.0(10)^5$	.33	$1.48(10)^5$	.288	$5.76(10)^8$	.22
8	$8.0(10)^5$	.33	$1.48(10)^8$	.288	$5.76(10)^8$	.22
9	$1.4(10)^6$	.33	$1.48(10)^8$	.288	$5.76(10)^8$	.22

TABLE I - Material Properties for Surface. Displacement Calculations

RUN NO.	DISPLACEMENT RATIO
1	.34
2	.34
3	.34
4	.34
5	.34
6	.34
7	.33
8	.33
9	.33

TABLE II - Ratio of Cavern Roof Center Displacement/Surface Well Head Displacement

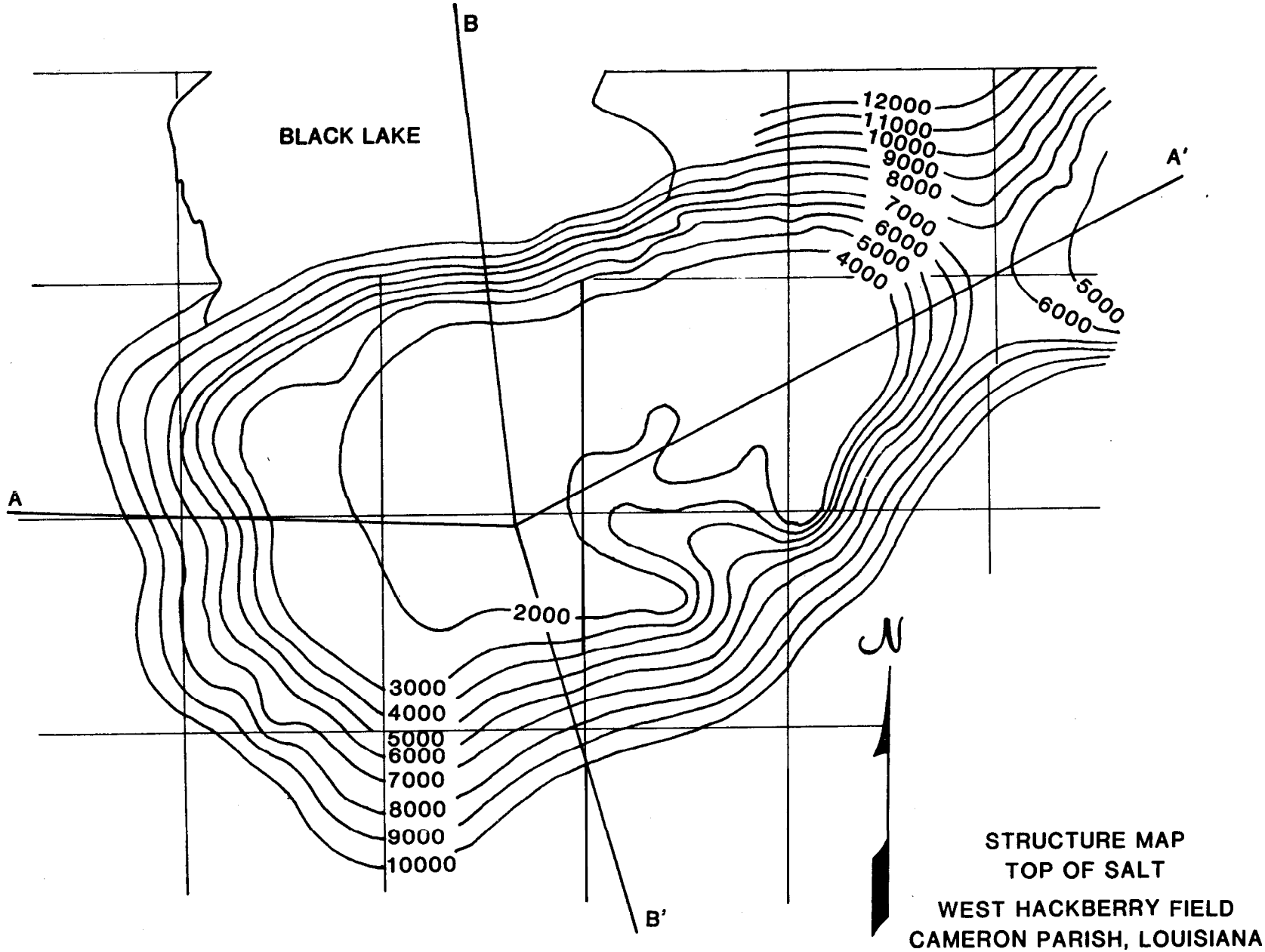

Figure 1 Map of West Hackberry Field

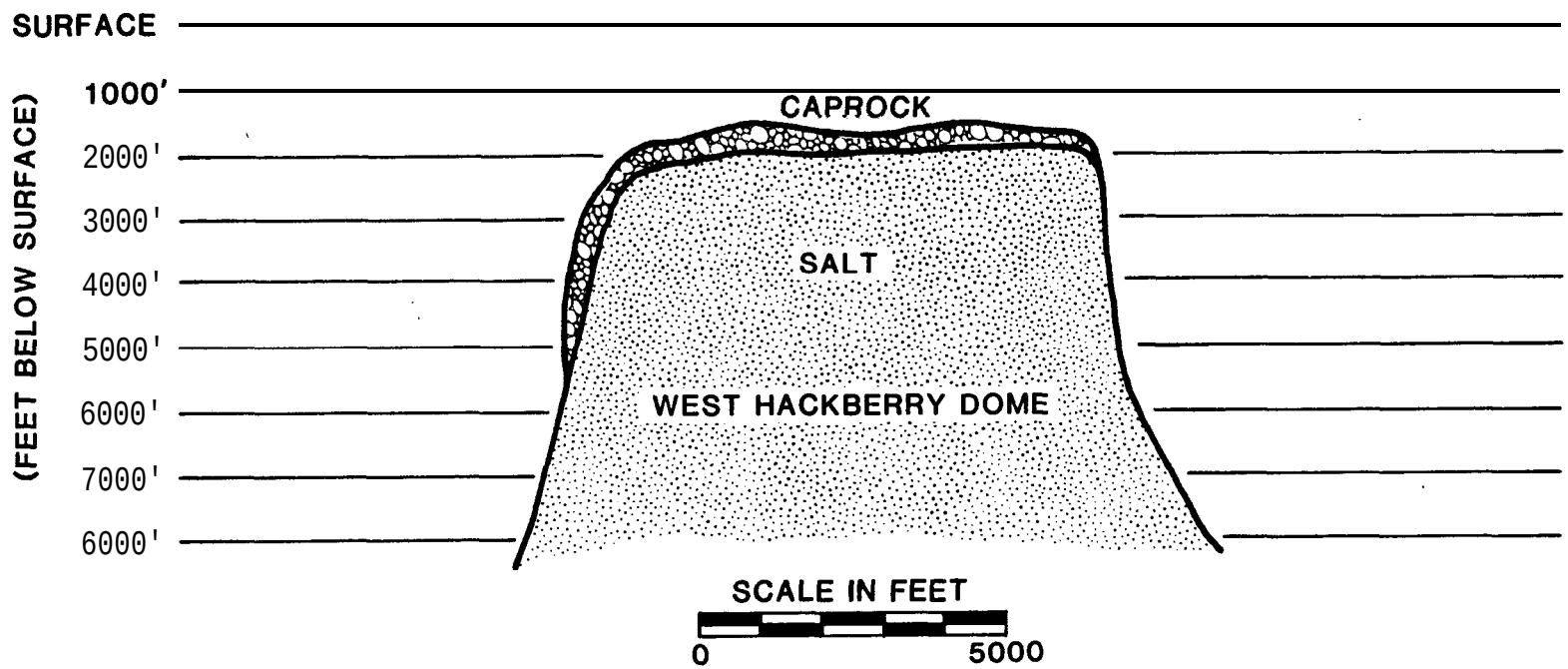

Figure 2 Cross-Section of West Hackberry Salt Dome

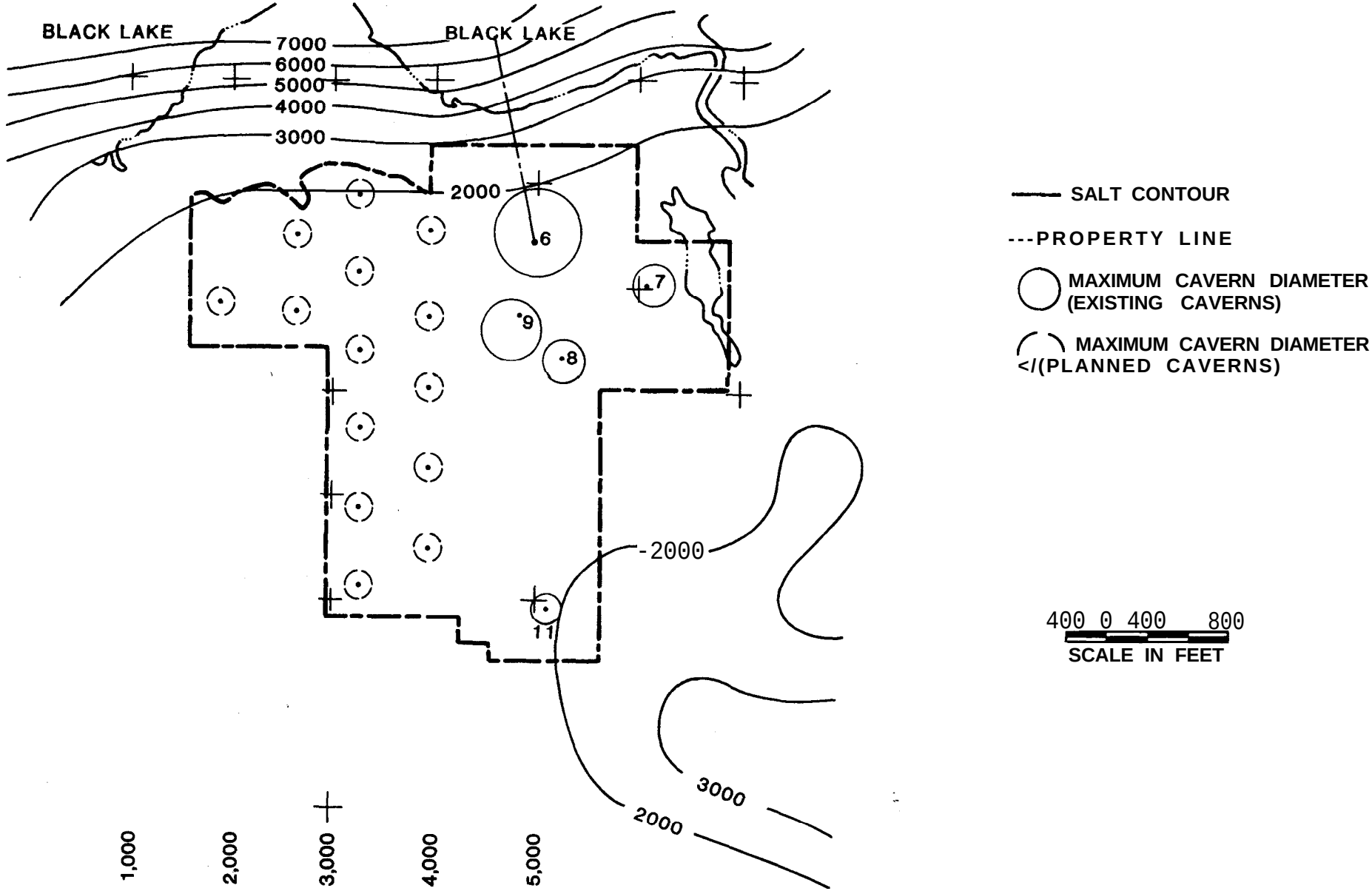

Figure 3 Plan View of Location of Cavern Number 6 in West Hackberry Field

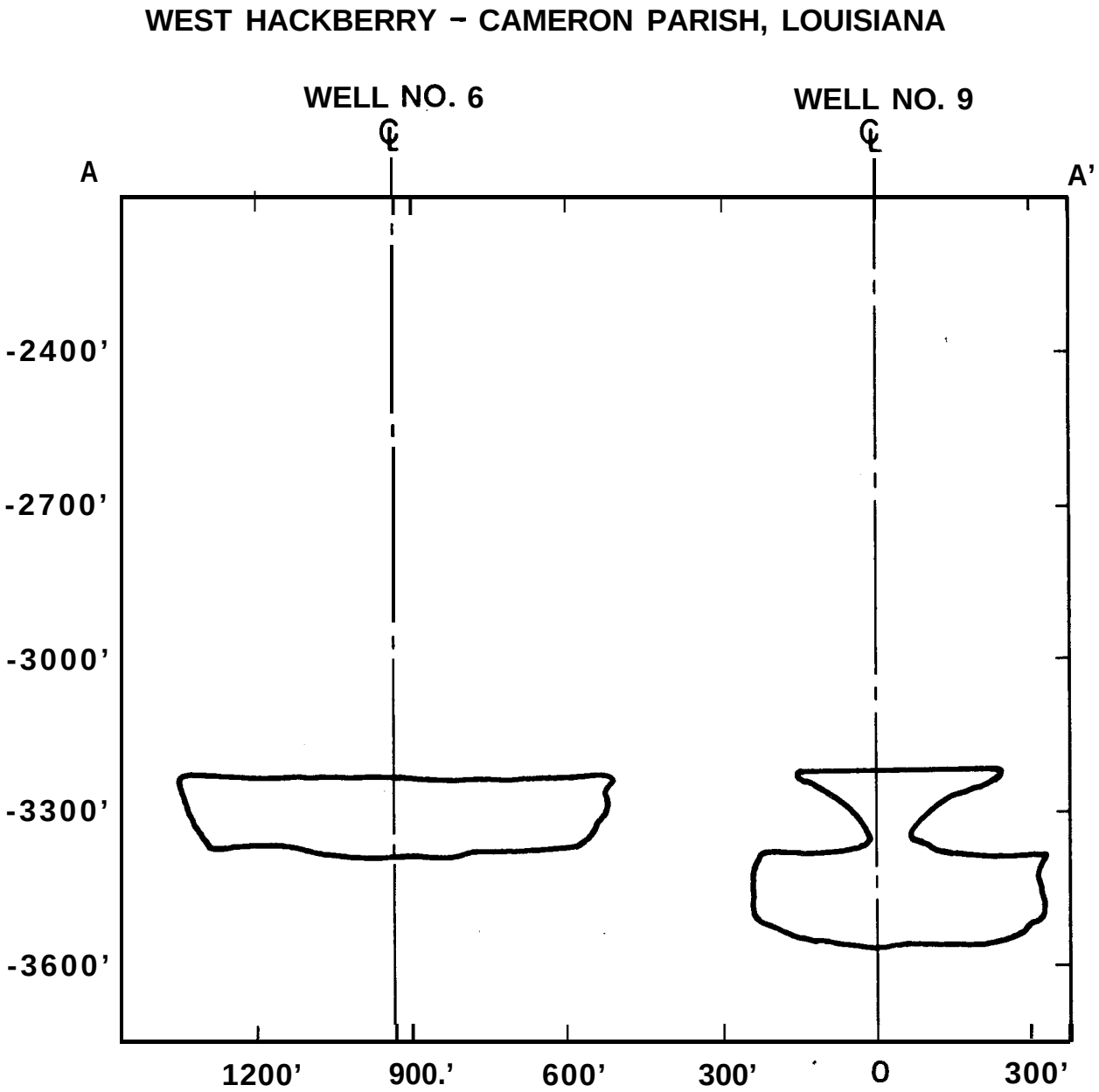

Figure 4 Cavern #6 Profile from Early Sonar Survey

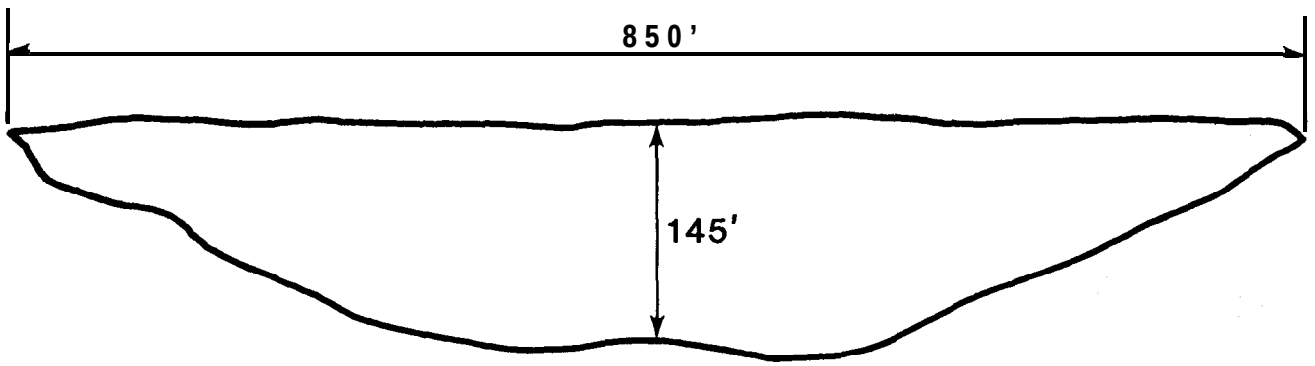

Figure 5 Recent Sonar Survey of WH6.

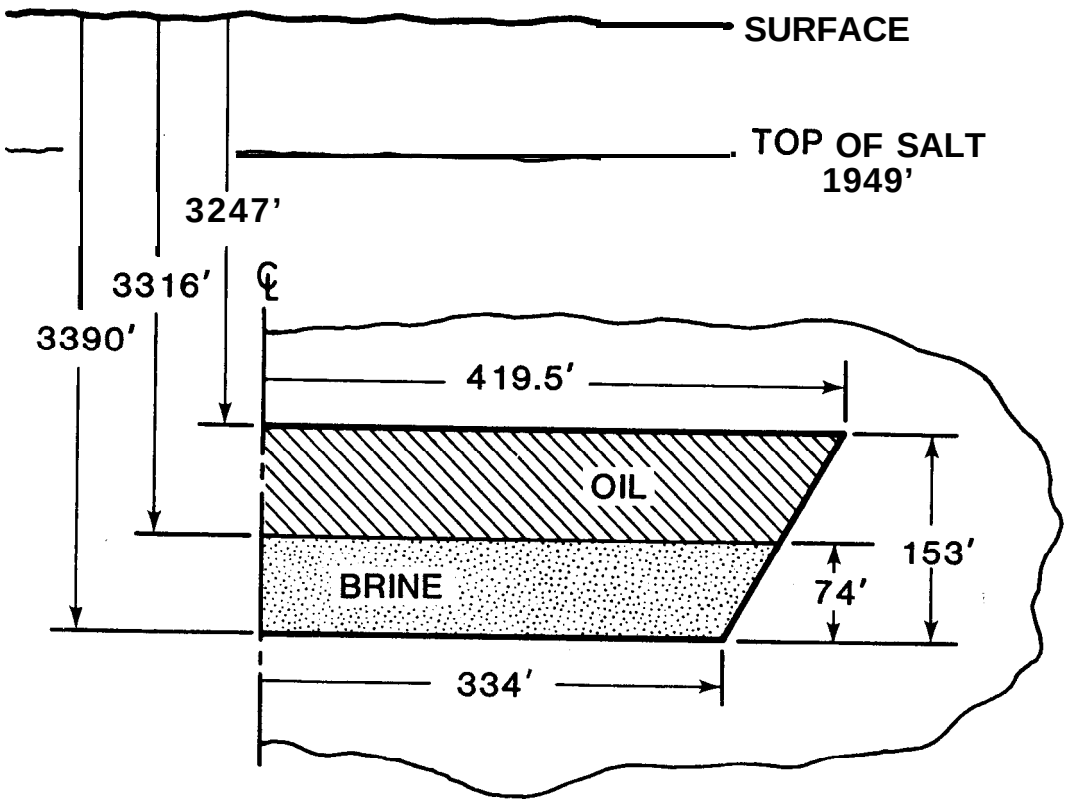

Figure 6 Schematic Diagram of **WH6.**

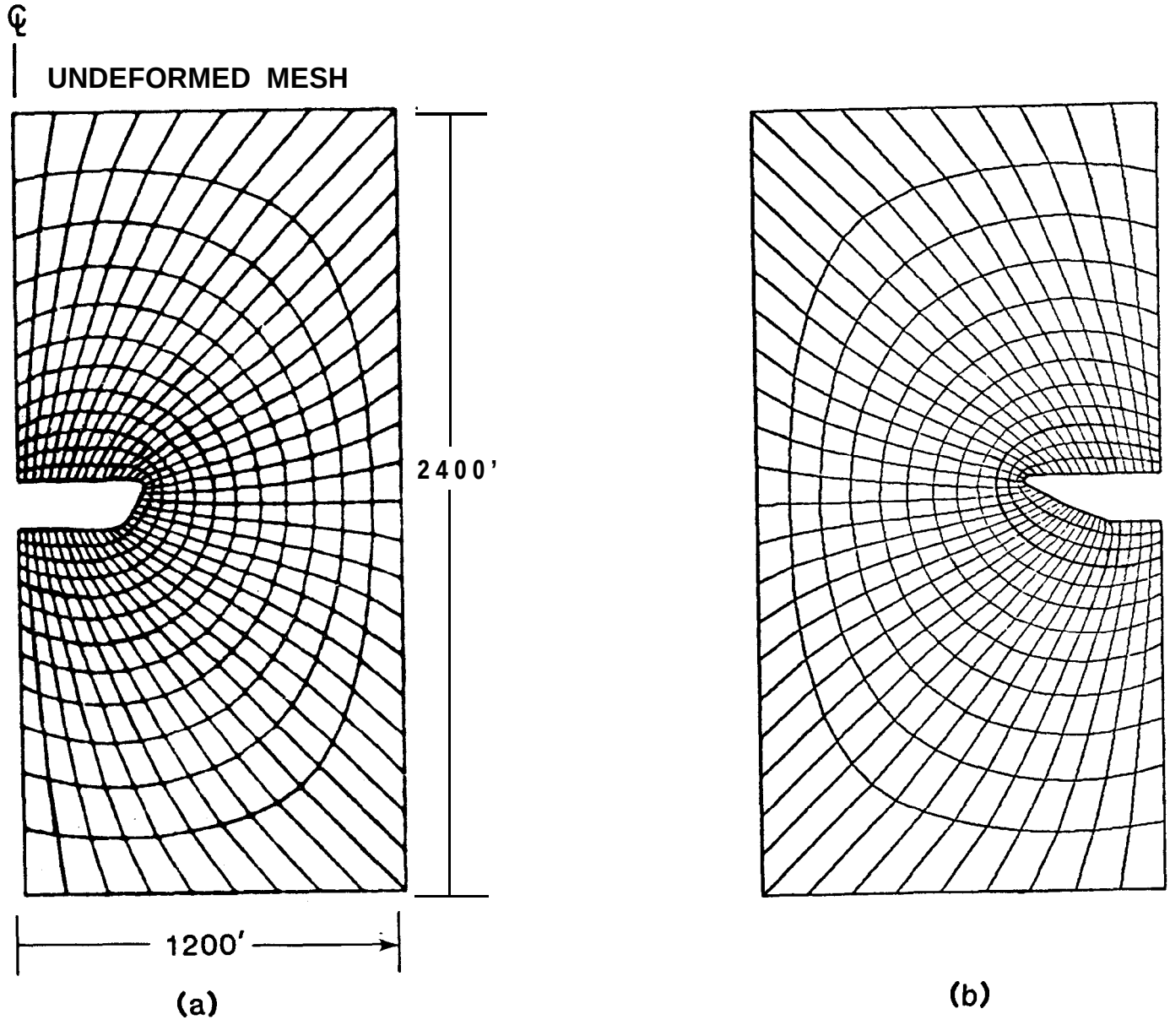

Figure 7 Finite Element Grids Used to Model WH6. a) Early Sonar Survey and b) Recent Sonar Survey

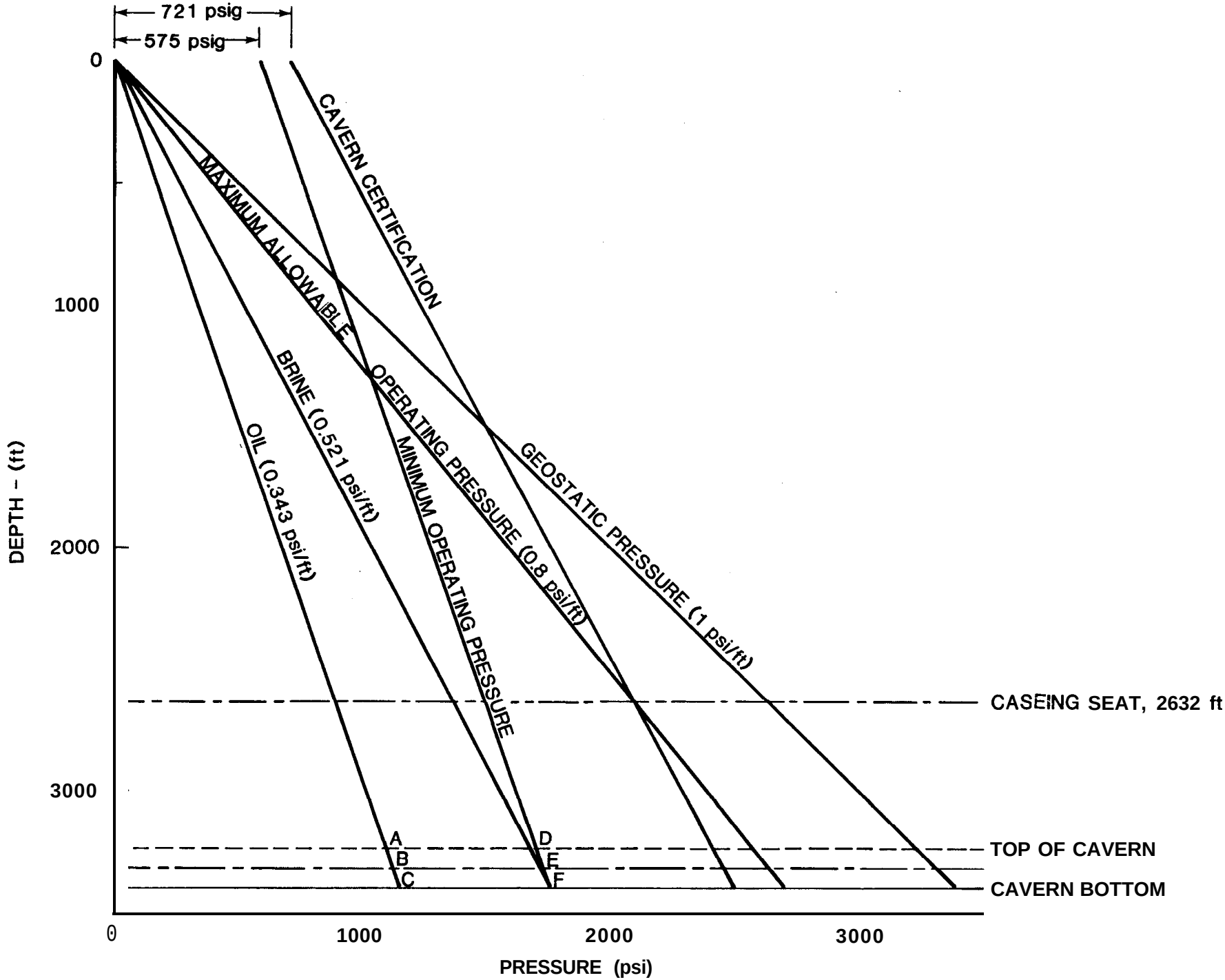

Figure 8 Loading Conditions for WH6.

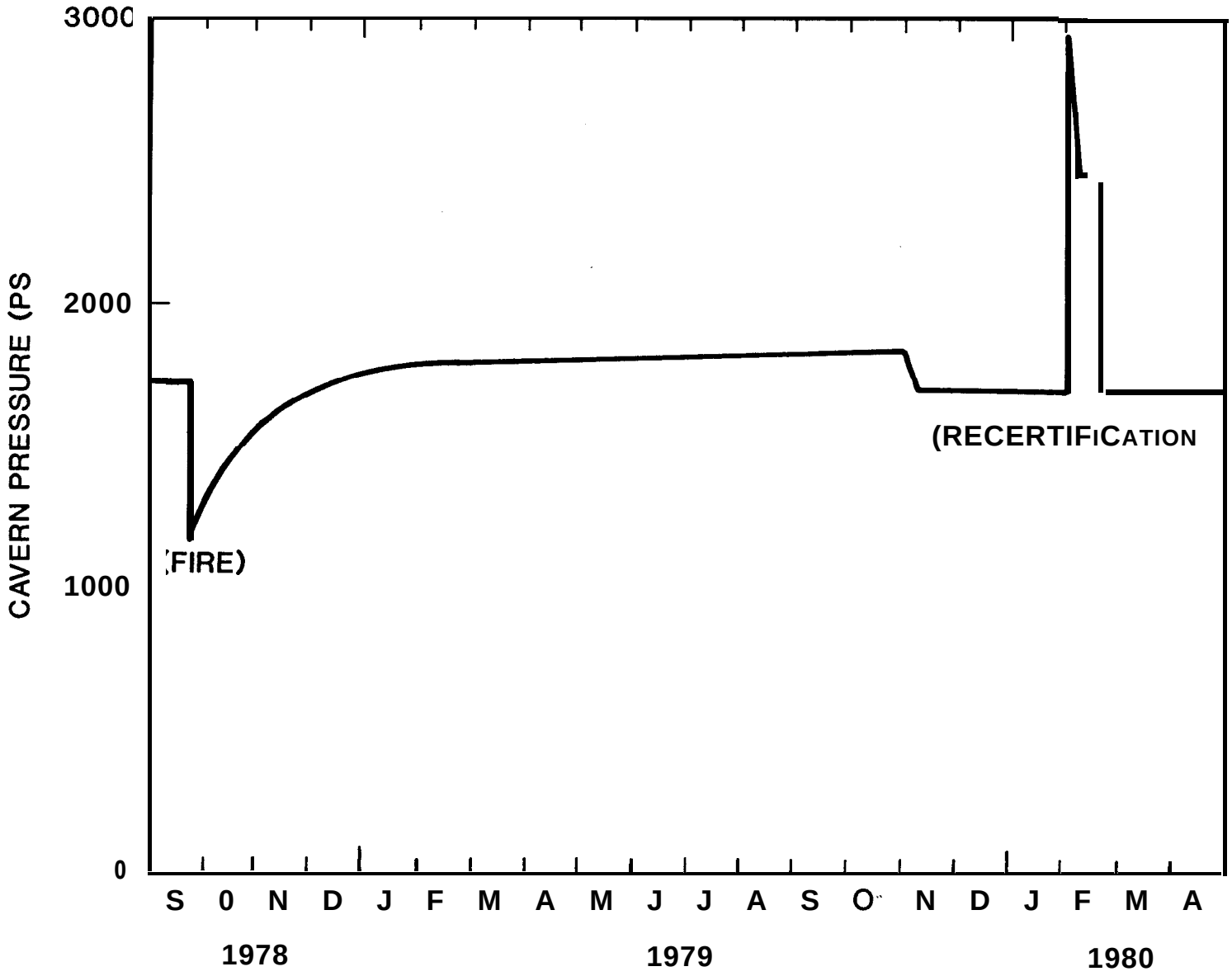

Figure 9 WH6 Loading History

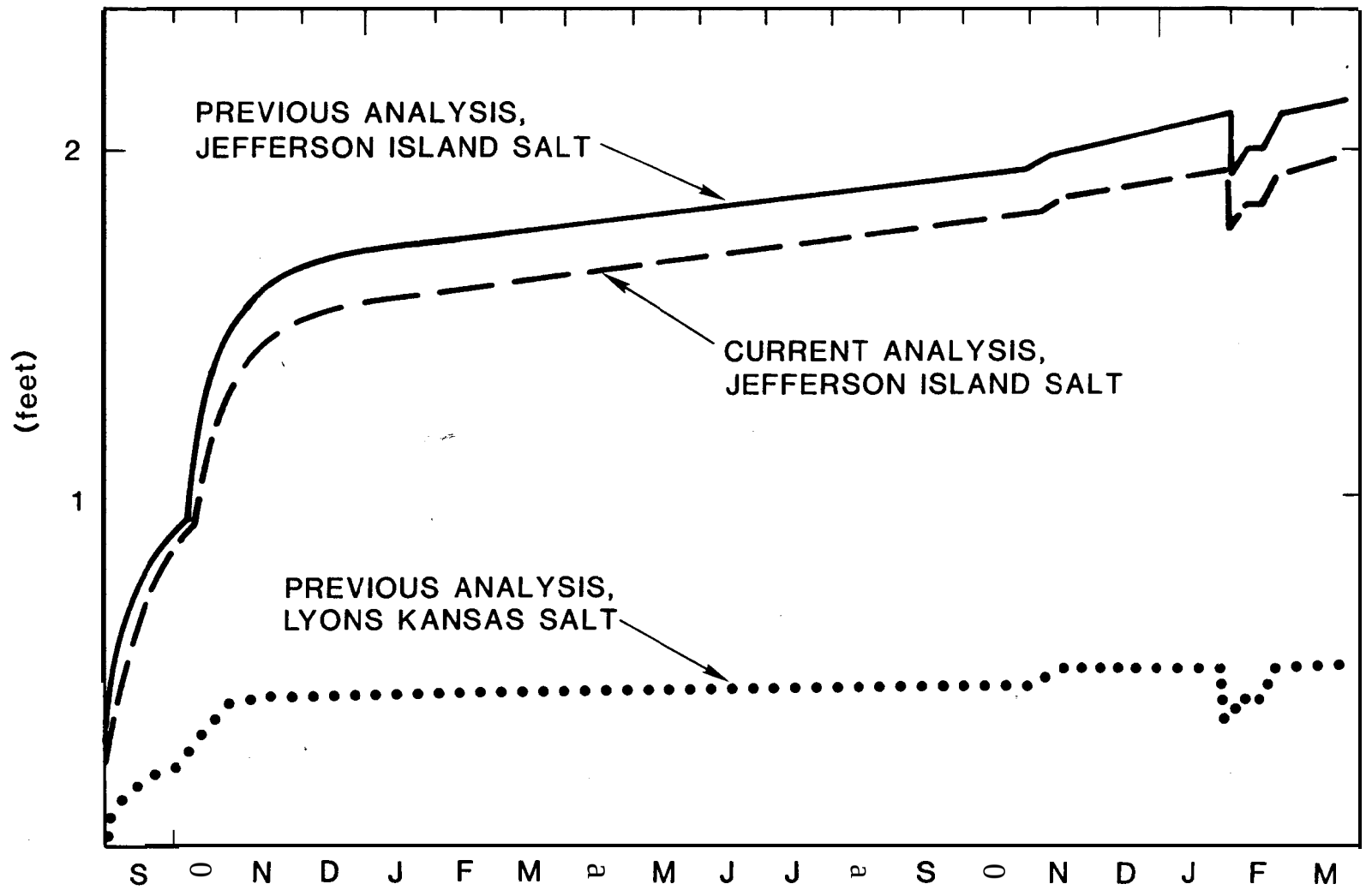

Figure 10 WH6 Roof Centerline Motion. Positive Motion Represents Cavern Closure.

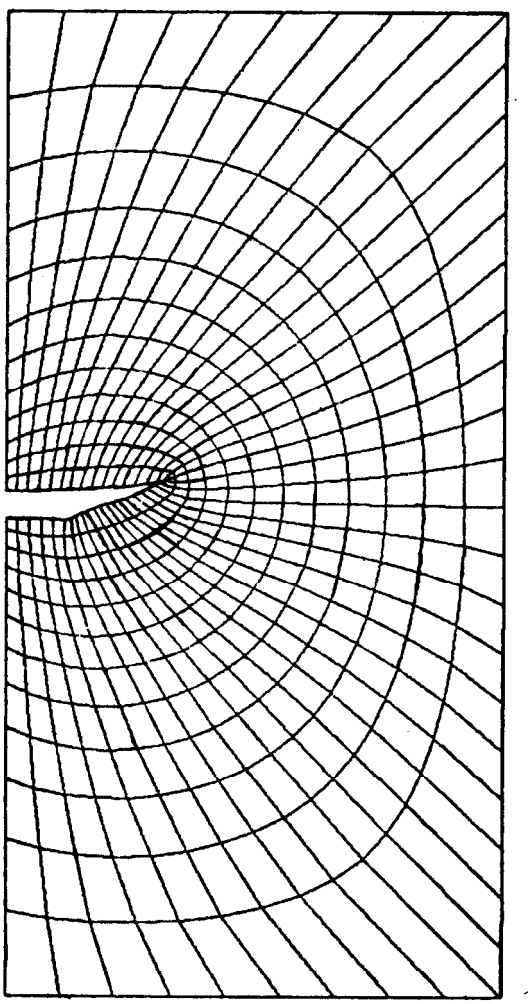

Figure 11

Magnitified Deformed Shape of WH6.

CREEP STRAIN CONTOURS (IN/IN)

A	0
B	0.01
C	0.03
D	0.05

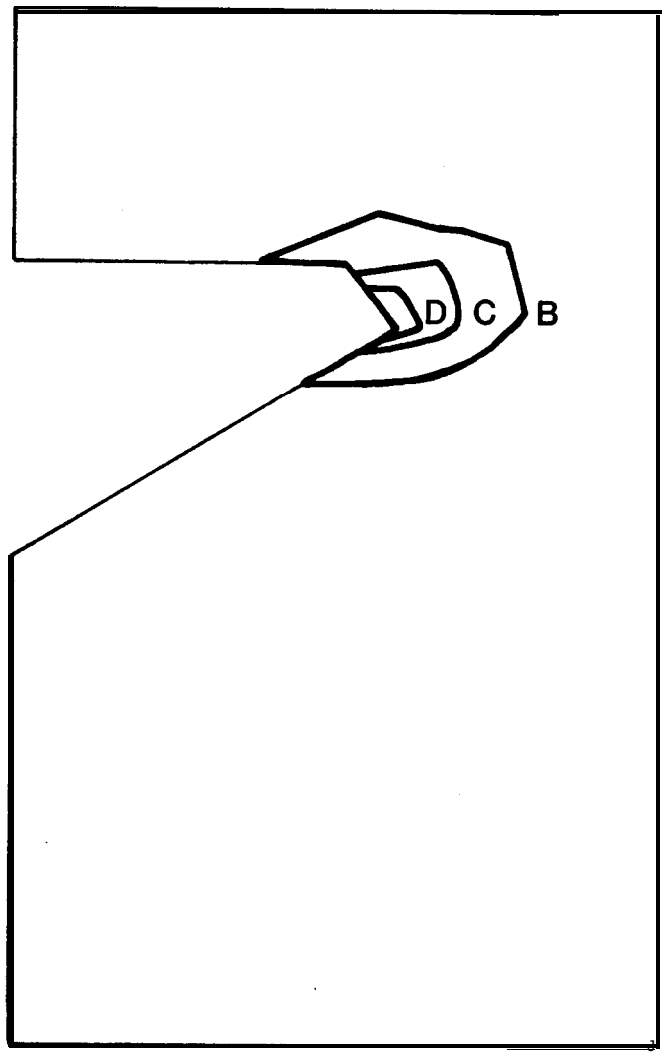

Figure 12

Creep Strain Contours Immediately After Recertification Test.

VON MISES STRESS
CONTOURS (PSI)
B - 277
C - 555
D - 833

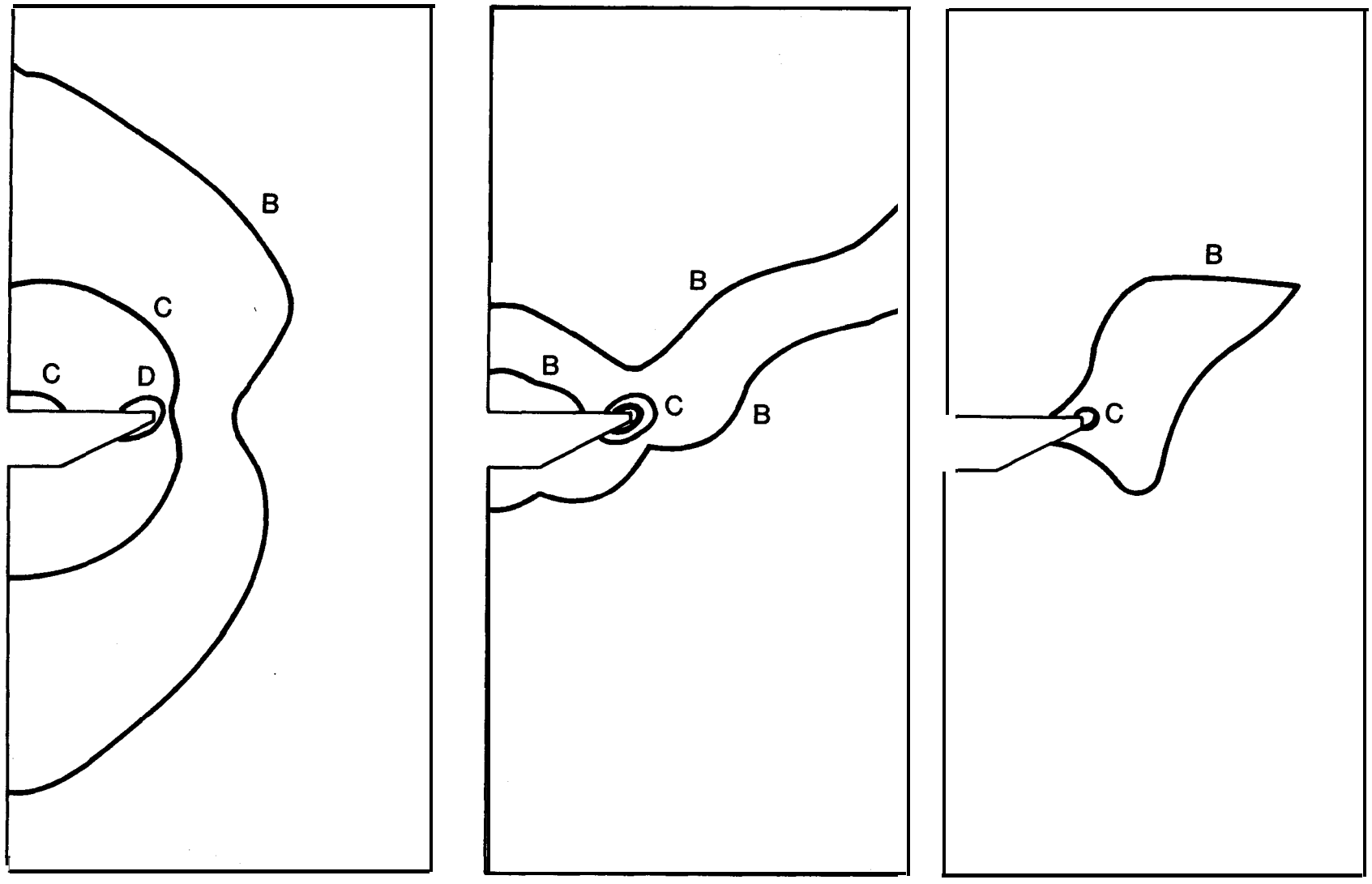

Figure 13 Von Mises Stress Contours: a) Before Recertification Pressure, b) At Maximum Recertification Pressure, c) At Secondary Recertification Pressure.

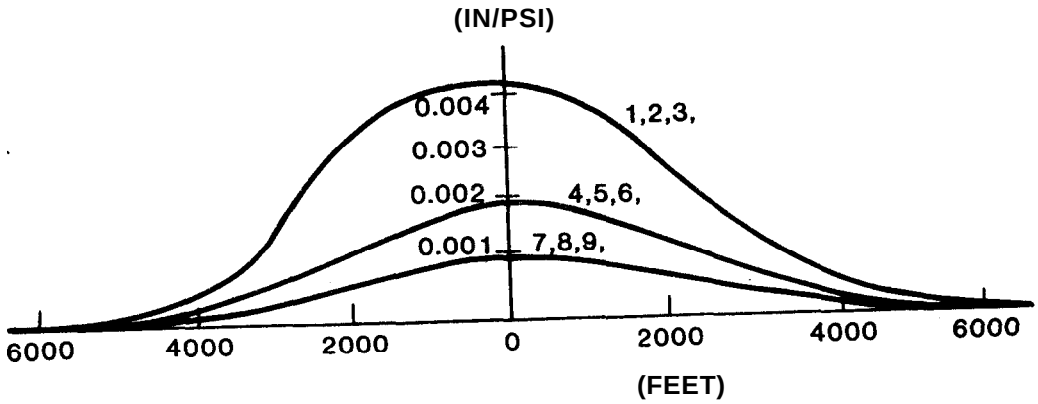

SURFACE UPLIFT

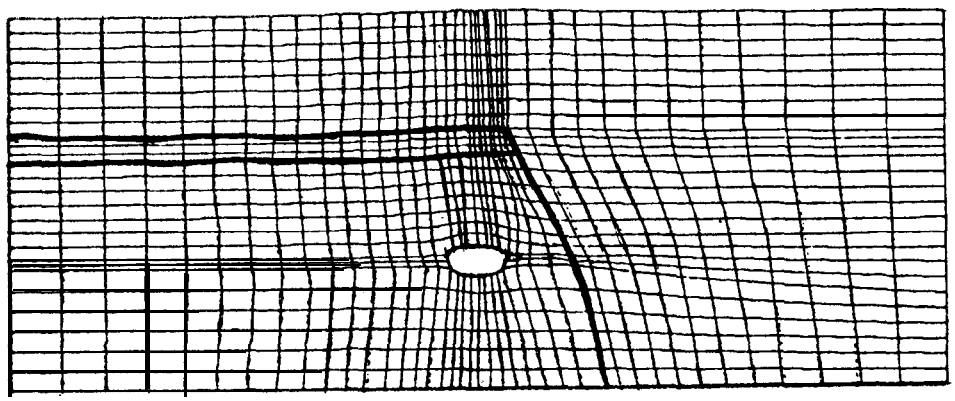

DEFORMED MESH

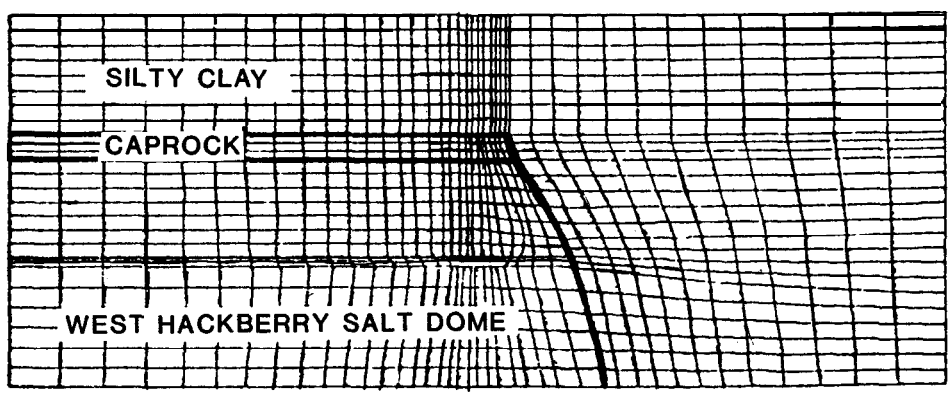

ORIGINAL MESH

Figure 14 Surface Uplift for WH6. Numbers 1 - 6 in Upper Figure Refer to Run Numbers Listed in Table I.

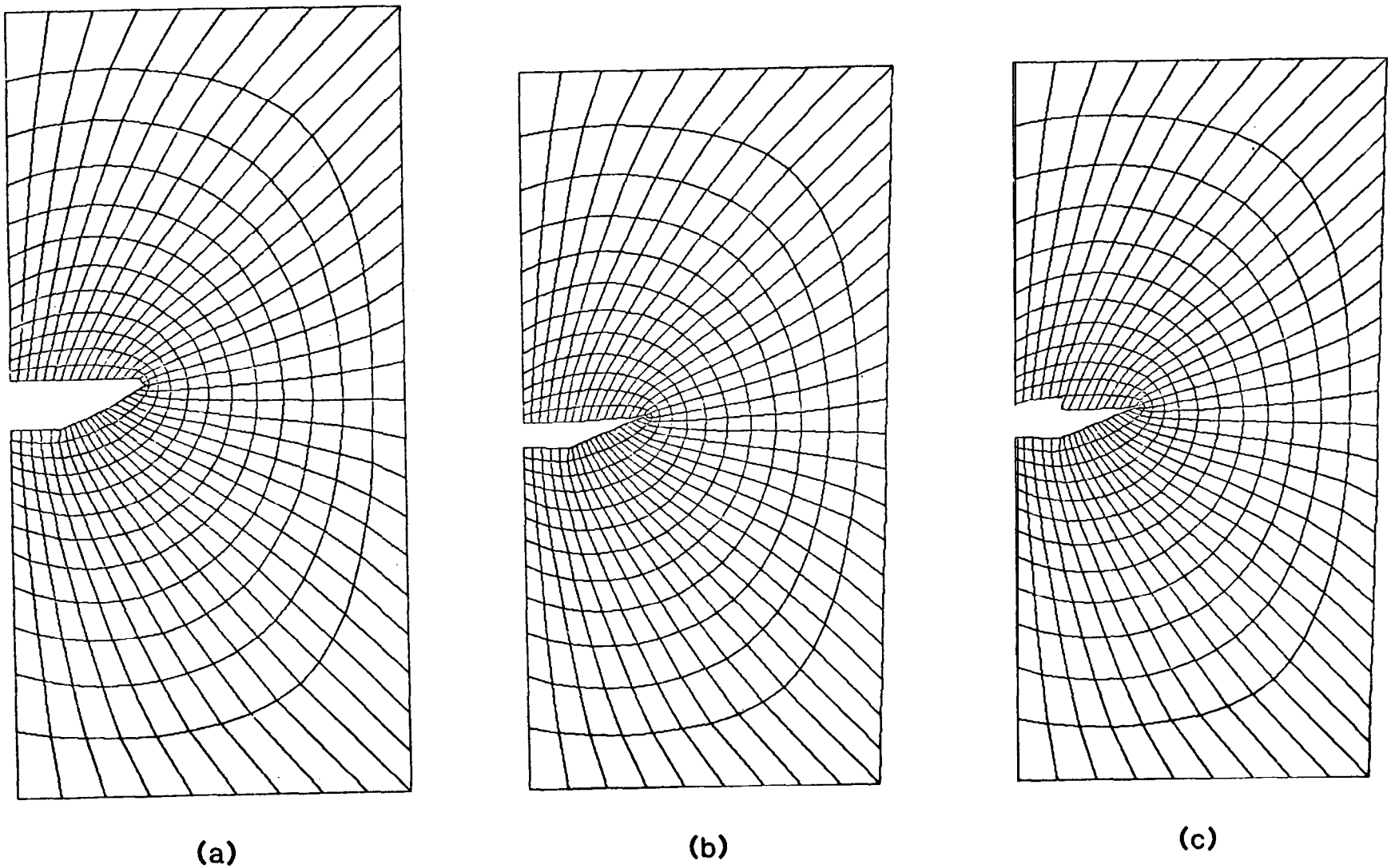

Figure 15 Undeformed and Magnified Deformed Shapes of Slabbing Calculation: a) Undeformed Grid, b) Deformed Grid Prior to Slabbing, c) Deformed Grid After Slabbing. Magnification Factor = 179.

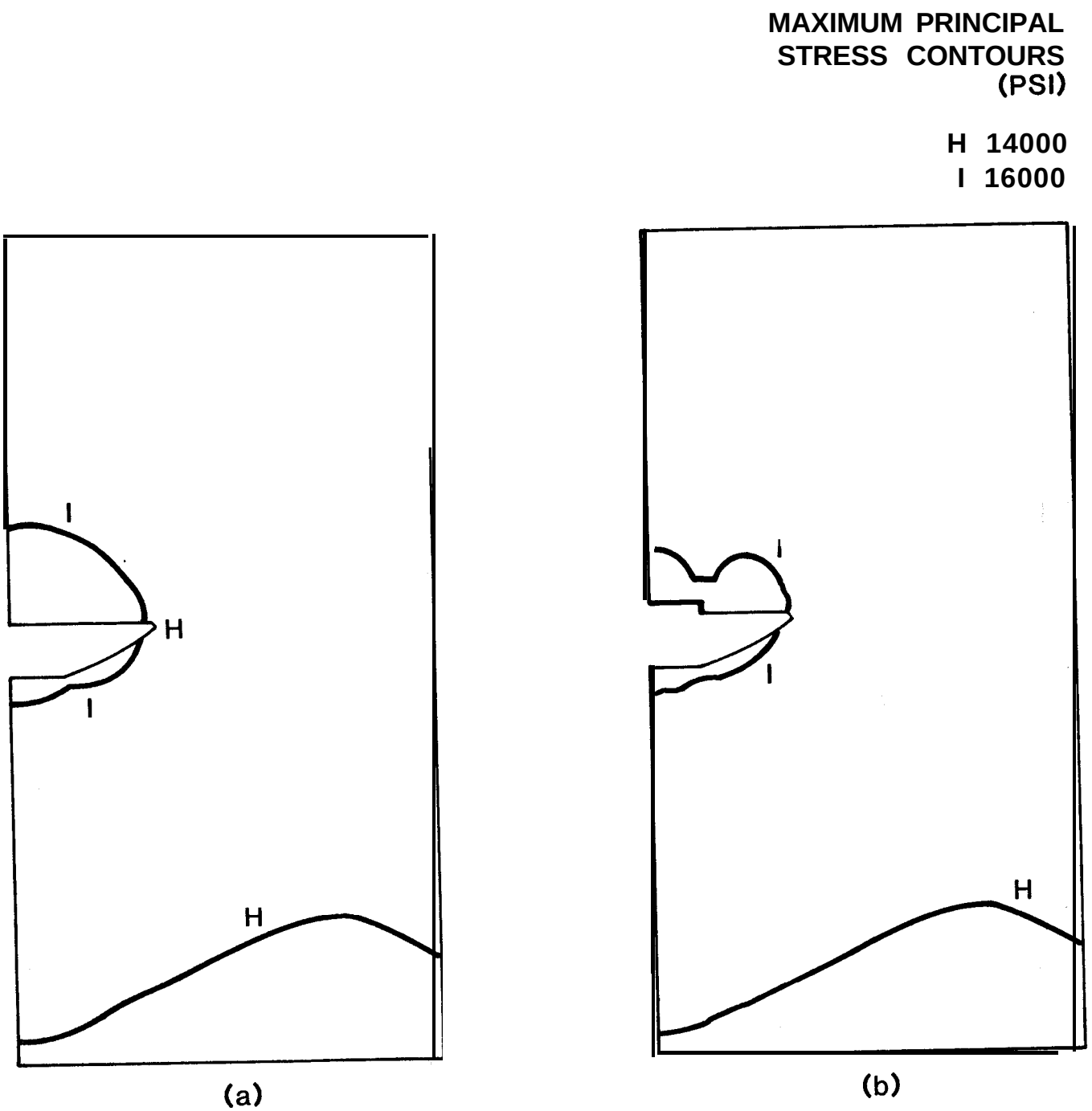

Figure 16 Maximum Principal Stress Contour Plots of Slabbing Simulation, a) Prior to Slabbing and b) After Slabbing.

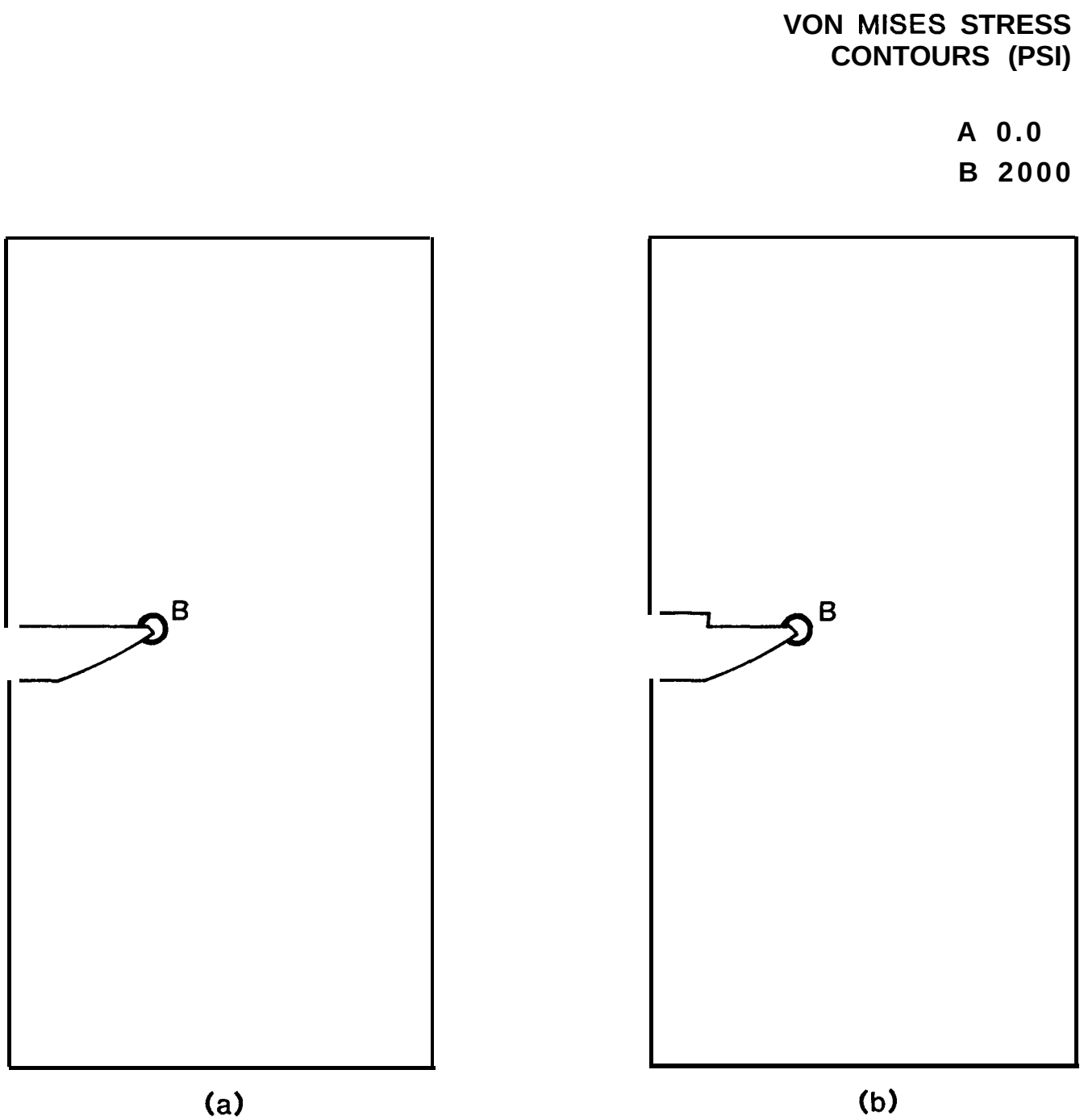

Figure 17 Von Mises Stress Contour Plots of Slabbing Simulation: a) Prior to Slabbing and b) After Slabbing.

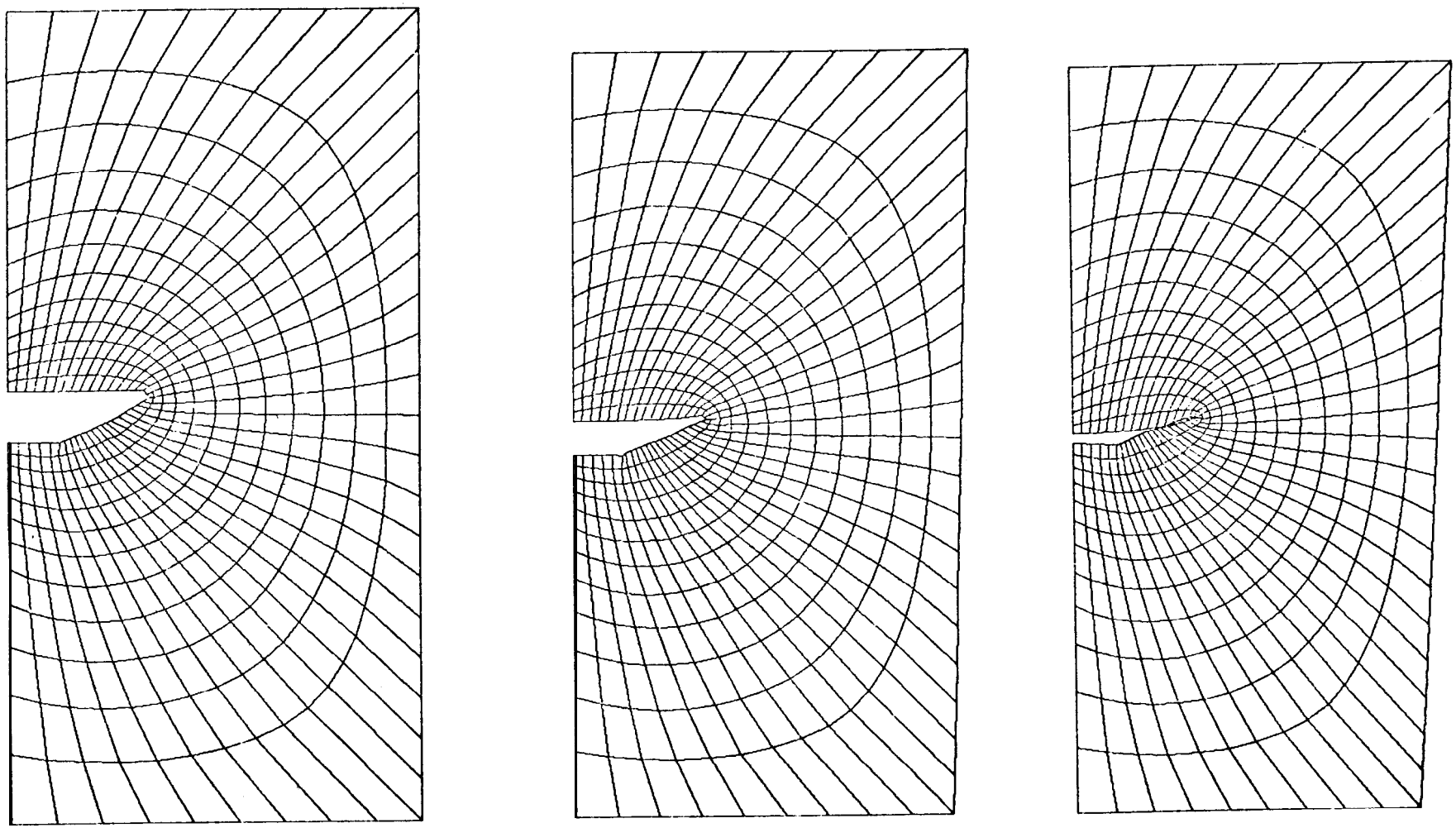

Figure 18 Undeformed and Magnified Deformed Shapes of Possible Accident Condition: a) Undeformed Shape, b) Magnified Deformed Shape with Cavern at Brine Head, c) Magnified Deformed Shape with Cavern at oil Head. Magnification Factor = 123.

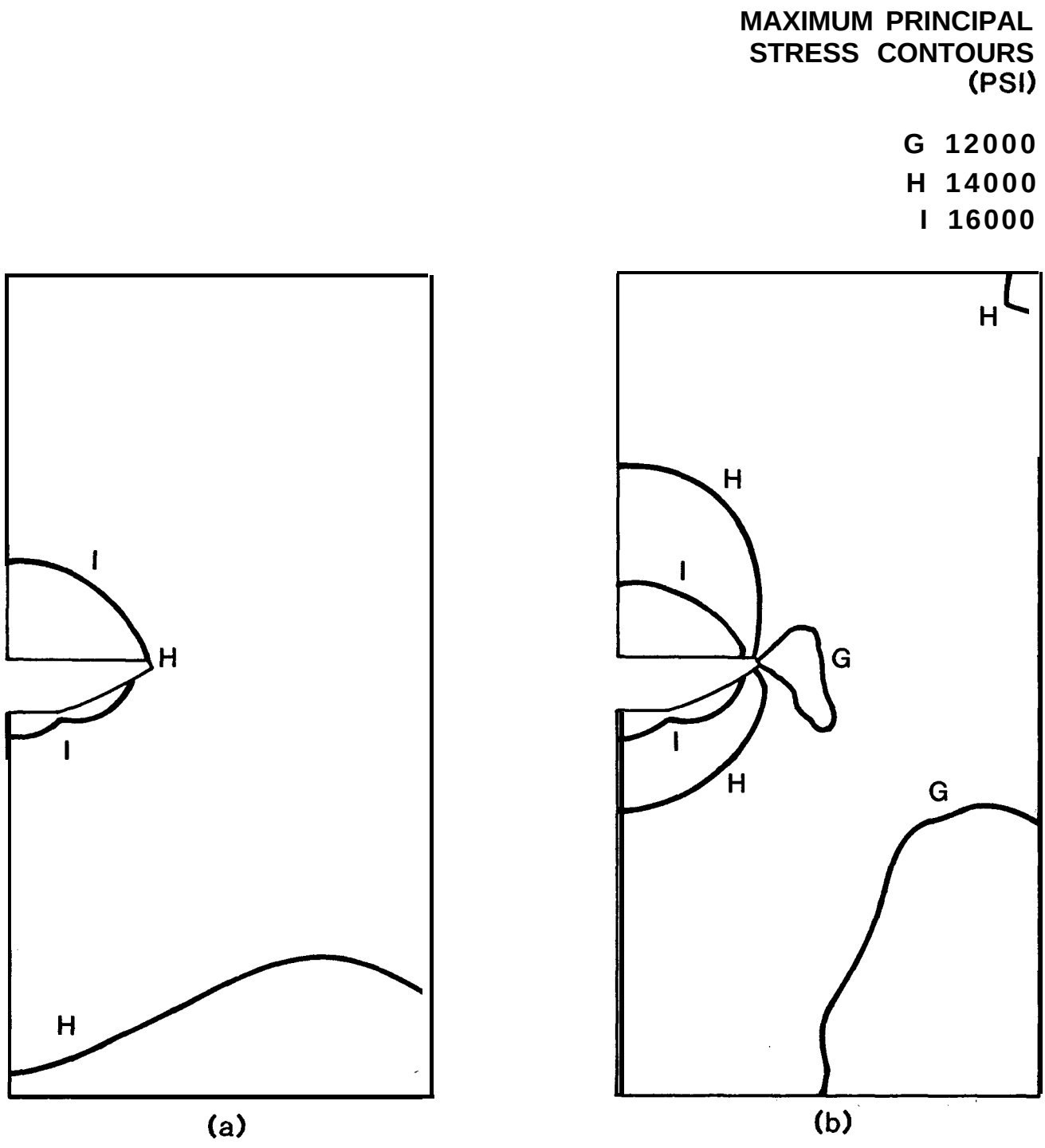

Figure 19 Maximum Principal Stress Contour Plots of Possible Accident Situation: a) Cavern at Brine Head and b) Cavern at oil Head.

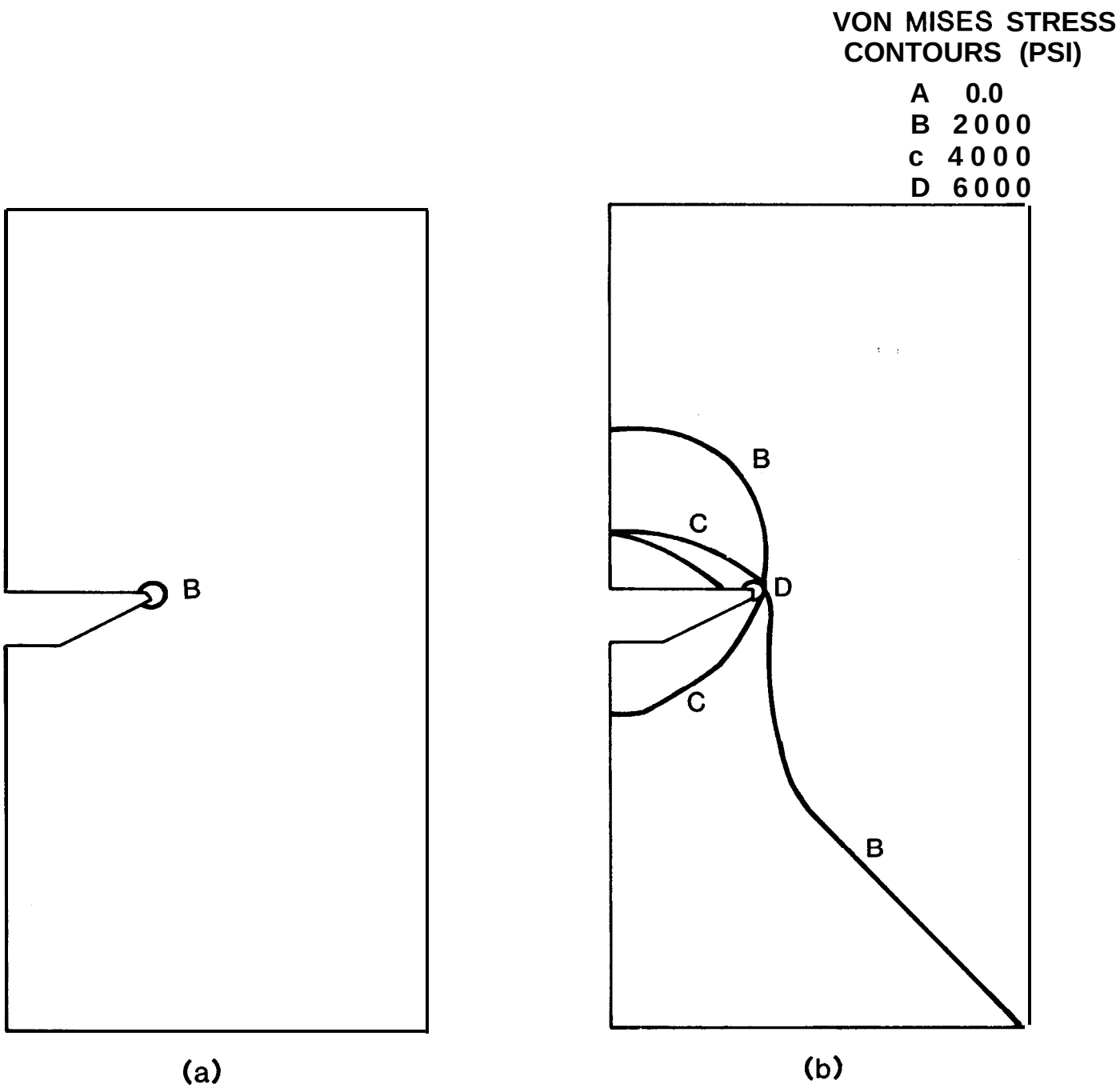

Figure 20 Von Mises Stress Contour Plots of Possible Accident Situation: a) Cavern at Brine Head and b) Cavern at oil Head.

Distribution:

U. S. Department of Energy
Strategic Petroleum Reserve
Project Management Office
900 Commerce Road East
New Orleans, LA 70123
Attn: C. C. Johnson
R. W. Mazurkiewicz (5)
G. J. Scango
G. A. Stafford

U. S. Department of Energy
Strategic Petroleum Reserve
1726 M Street N. W.
Washington, D. C. 20461
Attn: Larry Pettis

U. S. Department of Energy
Albuquerque Operations Office
P. 0. Box 5400
Albuquerque, N. M. 87115
Attn: D. C. Graves
C. B. Quinn

U. S. Army Corps of Engineers
900 Commerce Road East
New Orleans, LA 70123
Attn: Leo Carden

Aerospace Corporation
800 Commerce Road East
Suite 310
New Orleans, LA 70123
Attn: Elliott Katz

Parsons, Gilbane
800 Commerce Road West
New Orleans, LA 70123
Attn: Walter Marquardt

Dravo Utility Constructors, Inc.
850 S. Clearview Pkwy.
New Orleans, LA 70123
Attn: C. Ashline

Jacobs/D' appolonia Engineers
6226 Jefferson Hwy., Suite B
New Orleans, LA 70123
Attn: Harold Kubicek
c/o Bill Walker .

The Aerospace Corporation
P. 0. Box 92957
El Segundo, California
Los Angeles, California 90009
Attn: Guy F. Kuncir, Director

Arthur D. Little, Inc.
Acorn Park
Cambridge, Mass. 02140
Attn: P. D. Hilton

1100 G. A. Fowler
1100 C. D. Broyles
1120 T. L. Pace
1125 G. L. Ogle
1700 W. C. Myre
Attn: C. H. Mauney, 1720
J. D. Williams, 1729
4000 A. Narath
4500 E. H. Beckner
4540 M. L. Kramm
4541 L. w. Scully
4542 J. W. McKiernan
4543 J. F. Ney (10)
4543 M. H. Gubbels
4745 J. R. Tillerson
5000 J. K. Galt
5500 0. E. Jones
5510 D. B. Hayes
Attn: D. F. McVey, 5511
5520 T. B. Lane
5522 T. G. Priddy
5522 S. E. Benzley (5)
5530 W. Herrmann
5531 S. W. Key
5532 B. M. Butcher
5800 R. S. Claassen
5820 R. E. Whan
Attn: N. E. Brown, 5821
3141 T. L. Werner (5)
for DOE/TIC (Unlimited Release)
DOE/TIC (25)
R. P. Campbell, 3154-3
3151 W. L.,Garner (3)
8266 E. A. Aas